Upper Limits on a Stochastic Background of Gravitational Waves

B. Abbott,[12] R. Abbott,[12] R. Adhikari,[12] J. Agresti,[12] P. Ajith,[2] B. Allen,[37] J. Allen,[13] R. Amin,[16] S. B. Anderson,[12] W. G. Anderson,[37] M. Araya,[12] H. Armandula,[12] M. Ashley,[26] C. Aulbert,[1] S. Babak,[1] R. Balasubramanian,[7] S. Ballmer,[13] B. C. Barish,[12] C. Barker,[14] D. Barker,[14] M. A. Barton,[12] K. Bayer,[13] K. Belczynski,[22,*] J. Betzwieser,[13] B. Bhawal,[12] I. A. Bilenko,[19] G. Billingsley,[12] E. Black,[12] K. Blackburn,[12] L. Blackburn,[13] B. Bland,[14] L. Bogue,[15] R. Bork,[12] S. Bose,[39] P. R. Brady,[37] V. B. Braginsky,[19] J. E. Brau,[35] D. A. Brown,[12] A. Buonanno,[6] D. Busby,[12] W. E. Butler,[36] L. Cadonati,[13] G. Cagnoli,[33] J. B. Camp,[20] J. Cannizzo,[20] K. Cannon,[37] L. Cardenas,[12] K. Carter,[15] M. M. Casey,[33] P. Charlton,[12,†] S. Chatterji,[12] Y. Chen,[1] D. Chin,[34] N. Christensen,[8] T. Cokelaer,[7] C. N. Colacino,[31] R. Coldwell,[32] D. Cook,[14] T. Corbitt,[13] D. Coyne,[12] J. D. E. Creighton,[37] T. D. Creighton,[12] J. Dalrymple,[25] E. D'Ambrosio,[12] K. Danzmann,[29,2] G. Davies,[7] D. DeBra,[24] V. Dergachev,[34] S. Desai,[26] R. DeSalvo,[12] S. Dhurandar,[11] M. Díaz,[27] A. Di Credico,[25] R. W. P. Drever,[4] R. J. Dupuis,[12] P. Ehrens,[12] T. Etzel,[12] M. Evans,[12] T. Evans,[15] S. Fairhurst,[37] L. S. Finn,[26] K. Y. Franzen,[32] R. E. Frey,[35] P. Fritschel,[13] V. V. Frolov,[15] M. Fyffe,[15] K. S. Ganezer,[5] J. Garofoli,[14] I. Gholami,[1] J. A. Giaime,[16] K. Goda,[13] L. Goggin,[12] G. González,[16] C. Gray,[14] A. M. Gretarsson,[15] D. Grimmett,[12] H. Grote,[2] S. Grunewald,[1] M. Guenther,[14] R. Gustafson,[34] W. O. Hamilton,[16] C. Hanna,[16] J. Hanson,[15] C. Hardham,[24] G. Harry,[13] J. Heefner,[12] I. S. Heng,[33] M. Hewitson,[2] N. Hindman,[14] P. Hoang,[12] J. Hough,[33] W. Hua,[24] M. Ito,[35] Y. Itoh,[37] A. Ivanov,[12] B. Johnson,[14] W. W. Johnson,[16] D. I. Jones,[26,‡] G. Jones,[7] L. Jones,[12] V. Kalogera,[22] E. Katsavounidis,[13] K. Kawabe,[14] S. Kawamura,[21] W. Kells,[12] A. Khan,[15] C. Kim,[22] P. King,[12] S. Klimenko,[32] S. Koranda,[37] D. Kozak,[12] B. Krishnan,[1] M. Landry,[14] B. Lantz,[24] A. Lazzarini,[12] M. Lei,[12] I. Leonor,[35] K. Libbrecht,[12] P. Lindquist,[12] S. Liu,[12] M. Lormand,[15] M. Lubinski,[14] H. Lück,[29,2] M. Luna,[30] B. Machenschalk,[1] M. MacInnis,[13] M. Mageswaran,[12] K. Mailand,[12] M. Malec,[29] V. Mandic,[12] S. Marka,[9] E. Maros,[12] K. Mason,[13] L. Matone,[9] N. Mavalvala,[13] R. McCarthy,[14] D. E. McClelland,[3] M. McHugh,[18] J. W. C. McNabb,[26] A. Melissinos,[36] G. Mendell,[14] R. A. Mercer,[31] S. Meshkov,[12] E. Messaritaki,[37] C. Messenger,[31] E. Mikhailov,[13] S. Mitra,[11] V. P. Mitrofanov,[19] G. Mitselmakher,[32] R. Mittleman,[13] O. Miyakawa,[12] S. Mohanty,[27] G. Moreno,[14] K. Mossavi,[2] G. Mueller,[32] S. Mukherjee,[27] E. Myers,[38] J. Myers,[14] T. Nash,[12] F. Nocera,[12] J. S. Noel,[39] B. O'Reilly,[15] R. O'Shaughnessy,[22] D. J. Ottaway,[13] H. Overmier,[15] B. J. Owen,[26] Y. Pan,[6] M. A. Papa,[1] V. Parameshwaraiah,[14] C. Parameswariah,[15,§] M. Pedraza,[12] S. Penn,[10] M. Pitkin,[33] R. Prix,[1] V. Quetschke,[32] F. Raab,[14] H. Radkins,[14] R. Rahkola,[35] M. Rakhmanov,[32] K. Rawlins,[13] S. Ray-Majumder,[37] V. Re,[31] T. Regimbau,[7,‖] D. H. Reitze,[32] R. Riesen,[15] K. Riles,[34] B. Rivera,[14] D. I. Robertson,[33] N. A. Robertson,[24,33] C. Robinson,[7] S. Roddy,[15] A. Rodriguez,[16] J. Rollins,[9] J. D. Romano,[7] J. Romie,[12] S. Rowan,[33] A. Rüdiger,[2] L. Ruet,[13] P. Russell,[12] K. Ryan,[14] V. Sandberg,[14] G. H. Sanders,[12,¶] V. Sannibale,[12] P. Sarin,[13] B. S. Sathyaprakash,[7] P. R. Saulson,[25] R. Savage,[14] A. Sazonov,[32] R. Schilling,[2] R. Schofield,[35] B. F. Schutz,[1] P. Schwinberg,[14] S. M. Scott,[3] S. E. Seader,[39] A. C. Searle,[3] B. Sears,[12] D. Sellers,[15] A. S. Sengupta,[7] P. Shawhan,[12] D. H. Shoemaker,[13] A. Sibley,[15] X. Siemens,[37] D. Sigg,[14] A. M. Sintes,[30,1] J. Smith,[2] M. R. Smith,[12] O. Spjeld,[15] K. A. Strain,[33] D. M. Strom,[35] A. Stuver,[26] T. Summerscales,[26] M. Sung,[16] P. J. Sutton,[12] D. B. Tanner,[32] R. Taylor,[12] K. A. Thorne,[26] K. S. Thorne,[6] K. V. Tokmakov,[19] C. Torres,[27] C. Torrie,[12] G. Traylor,[15] W. Tyler,[12] D. Ugolini,[28] C. Ungarelli,[31] M. Vallisneri,[6] M. van Putten,[13] S. Vass,[12] A. Vecchio,[31] J. Veitch,[33] C. Vorvick,[14] S. P. Vyachanin,[19] L. Wallace,[12] H. Ward,[33] R. Ward,[12] K. Watts,[15] D. Webber,[12] U. Weiland,[29] A. Weinstein,[12] R. Weiss,[13] S. Wen,[16] K. Wette,[3] J. T. Whelan,[18] S. E. Whitcomb,[12] B. F. Whiting,[32] S. Wiley,[5] C. Wilkinson,[14] P. A. Willems,[12] B. Willke,[29,2] A. Wilson,[12] W. Winkler,[2] S. Wise,[32] A. G. Wiseman,[37] G. Woan,[33] D. Woods,[37] R. Wooley,[15] J. Worden,[14] I. Yakushin,[15] H. Yamamoto,[12] S. Yoshida,[23] M. Zanolin,[13] L. Zhang,[12] N. Zotov,[17] M. Zucker,[15] and J. Zweizig[12]

(LIGO Scientific Collaboration)

[1]*Albert-Einstein-Institut, Max-Planck-Institut für Gravitationsphysik, D-14476 Golm, Germany*
[2]*Albert-Einstein-Institut, Max-Planck-Institut für Gravitationsphysik, D-30167 Hannover, Germany*
[3]*Australian National University, Canberra, 0200, Australia*
[4]*California Institute of Technology, Pasadena, California 91125, USA*
[5]*California State University Dominguez Hills, Carson, California 90747, USA*
[6]*Caltech-CaRT, Pasadena, California 91125, USA*
[7]*Cardiff University, Cardiff, CF2 3YB, United Kingdom*
[8]*Carleton College, Northfield, Minnesota 55057, USA*
[9]*Columbia University, New York, New York 10027, USA*

[10]Hobart and William Smith Colleges, Geneva, New York 14456, USA
[11]Inter-University Centre for Astronomy and Astrophysics, Pune - 411007, India
[12]LIGO—California Institute of Technology, Pasadena, California 91125, USA
[13]LIGO—Massachusetts Institute of Technology, Cambridge, Massachusetts 02139, USA
[14]LIGO Hanford Observatory, Richland, Washington 99352, USA
[15]LIGO Livingston Observatory, Livingston, Louisiana 70754, USA
[16]Louisiana State University, Baton Rouge, Louisiana 70803, USA
[17]Louisiana Tech University, Ruston, Louisiana 71272, USA
[18]Loyola University, New Orleans, Louisiana 70118, USA
[19]Moscow State University, Moscow, 119992, Russia
[20]NASA/Goddard Space Flight Center, Greenbelt, Maryland 20771, USA
[21]National Astronomical Observatory of Japan, Tokyo 181-8588, Japan
[22]Northwestern University, Evanston, Illinois 60208, USA
[23]Southeastern Louisiana University, Hammond, Louisiana 70402, USA
[24]Stanford University, Stanford, California 94305, USA
[25]Syracuse University, Syracuse, New York 13244, USA
[26]The Pennsylvania State University, University Park, Pennsylvania 16802, USA
[27]The University of Texas at Brownsville and Texas Southmost College, Brownsville, Texas 78520, USA
[28]Trinity University, San Antonio, Texas 78212, USA
[29]Universität Hannover, D-30167 Hannover, Germany
[30]Universitat de les Illes Balears, E-07122 Palma de Mallorca, Spain
[31]University of Birmingham, Birmingham, B15 2TT, United Kingdom
[32]University of Florida, Gainesville, Florida 32611, USA
[33]University of Glasgow, Glasgow, G12 8QQ, United Kingdom
[34]University of Michigan, Ann Arbor, Michigan 48109, USA
[35]University of Oregon, Eugene, Oregon 97403, USA
[36]University of Rochester, Rochester, New York 14627, USA
[37]University of Wisconsin-Milwaukee, Milwaukee, Wisconsin 53201, USA
[38]Vassar College, Poughkeepsie, New York 12604, USA
[39]Washington State University, Pullman, Washington 99164, USA
(Received 30 July 2005; published 22 November 2005)

The Laser Interferometer Gravitational-Wave Observatory has performed a third science run with much improved sensitivities of all three interferometers. We present an analysis of approximately 200 hours of data acquired during this run, used to search for a stochastic background of gravitational radiation. We place upper bounds on the energy density stored as gravitational radiation for three different spectral power laws. For the flat spectrum, our limit of $\Omega_0 < 8.4 \times 10^{-4}$ in the 69–156 Hz band is $\sim 10^5$ times lower than the previous result in this frequency range.

DOI: 10.1103/PhysRevLett.95.221101 PACS numbers: 04.80.Nn, 04.30.Db, 07.05.Kf, 95.55.Ym

A stochastic background of gravitational waves could result from the random superposition of an extremely large number of unresolved and independent gravitational-wave (GW) emission events. Such a background is analogous to the cosmic microwave background radiation (CMBR), though its spectrum is unlikely to be thermal. The emission events could be the result of cosmological processes, as with the CMBR, but occurring much earlier after the big bang—e.g., during inflation. The events could also be due to more recent astrophysical processes. Placing upper limits on or detecting the energy density of a stochastic background of gravitational waves is one of the long-term goals of GW detectors.

The stochastic background spectrum is typically characterized in terms of a dimensionless quantity $\Omega_{\mathrm{GW}}(f)$: the GW energy density per unit logarithmic frequency, divided by the critical energy density ρ_c to close the Universe. The critical density, and thus $\Omega_{\mathrm{GW}}(f)$, depend on the Hubble expansion rate H_0; in this Letter, all bounds on $\Omega_{\mathrm{GW}}(f)$ will be for $H_0 = 72\ \mathrm{km\,sec^{-1}\,Mpc^{-1}}$ [1]. We search for power laws of the form $\Omega_{\mathrm{GW}}(f) = \Omega_\alpha (f/100\ \mathrm{Hz})^\alpha$. The choices of α are motivated by potential source models [2]: ($\alpha = 0$) predicted by inflationary or cosmic string models; ($\alpha = 2$) rotating neutron stars; ($\alpha = 3$) pre-big-bang cosmology.

Previous direct measurements of a stochastic background, in the ~ 10 Hz to $\sim 10^4$ Hz band accessible to Earth-based detectors, have been limited to establishing upper limits on $\Omega_{\mathrm{GW}}(f)$ greater than unity, with the best and most recent result using the Laser Interferometer Gravitational-Wave Observatory (LIGO)'s first science data finding $\Omega_0 < 44$ [3]. (The best upper limit from acoustic detectors is $\Omega_0 < 120$ at 907 Hz, from a cross-correlation measurement between the Explorer and Nautilus cryogenic bar detectors [4].) At much lower frequencies, spacecraft Doppler tracking has established

$\Omega_0 < 0.027$ in the band 10^{-6}–10^{-3} Hz [5], and radio pulsar timing has bounded $\Omega_0 < 10^{-7}$ in a decade band around 10^{-8} Hz [6]. In this Letter, we report new limits on a stochastic GW background for frequencies around 100 Hz, using data from the LIGO GW detectors. In terms of GW energy density, these limits are nearly 5 orders of magnitude below previous limits in this frequency band.

LIGO is composed of three GW interferometers at two sites: the 4 km H1 and 2 km H2 detectors, colocated at Hanford, WA, and the 4 km L1 detector, located in Livingston Parish, LA [7]. Each detector is a power-recycled Michelson interferometer, with 4 km (or 2 km) long Fabry-Perot cavities in each of its orthogonal arms. These interferometers are sensitive to quadrupolar oscillations in the space-time metric due to a passing GW, measuring directly the GW strain amplitude. While the detectors are still being commissioned to perform at their designed sensitivity, several dedicated data collection runs have been performed. The detector configuration and performance during LIGO's first science run (S1) is described in Ref. [8]. In this analysis, we use data from the third science run (S3), carried out from 31 October 2003–9 January 2004, with significantly improved sensitivity compared to previous runs. Figure 1 shows reference amplitude spectra of equivalent strain noise for S3.

To search for a stochastic background, we cross correlate the strain data from a pair of detectors, taking advantage of the fact that the instrumental noise of one interferometer will, in general, be uncorrelated with that of the other interferometers. This is more clearly the case for the widely separated interferometer pairs (i.e., L1 paired with H1 or H2), for which there are only a few paths through which instrumental correlations could arise. The H1-H2 cross correlation, on the other hand, is susceptible to a much broader range of potentially correlated instrumental noise sources. This Letter presents an analysis of the intersite pairs only; the H1-H2 measurement, though offering potentially higher sensitivity due to their collocation, requires additional techniques to address instrumental noise and may be presented in a later publication.

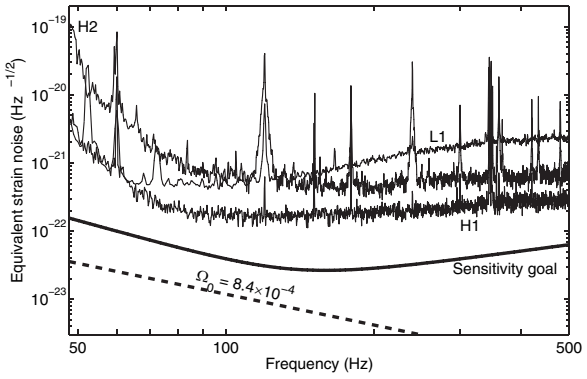

FIG. 1. Reference sensitivity curves during the S3 data run, in terms of equivalent strain noise density. Also shown is the $f^{-3/2}$ strain noise level corresponding to the upper limit found in this analysis, $\Omega_0 = 8.4 \times 10^{-4}$, and the strain noise goal for the two 4 km interferometers.

The cross correlation is performed in the frequency domain, using a linear filter that optimizes the expected signal-to-noise ratio, given the detectors' noise spectra and the targeted stochastic background (see Ref. [3] and references cited within). Specifically, with $\tilde{s}_1(f)$ and $\tilde{s}_2(f)$ representing the Fourier transforms of the strain outputs of two detectors, the cross correlation is computed as:

$$Y = \int_{-\infty}^{\infty} df \int_{-\infty}^{\infty} df' \delta_T(f - f') \tilde{s}_1^*(f) \tilde{Q}(f') \tilde{s}_2(f'), \quad (1)$$

where δ_T is a finite-time approximation to the Dirac delta function. The optimal filter $\tilde{Q}$ has the form:

$$\tilde{Q}(f) = \mathcal{N} \frac{\gamma(f) S_{\mathrm{GW}}(f)}{P_1(f) P_2(f)}, \quad (2)$$

where $\mathcal{N}$ is a normalization factor, P_1 and P_2 are the strain noise power spectra of the two detectors, S_{GW} is the strain power spectrum of the stochastic background being searched for $[S_{\mathrm{GW}}(f) = (3H_0^2/10\pi^2) f^{-3} \Omega_{\mathrm{GW}}(f)]$, and the factor γ is called the overlap reduction function [9]. This factor, defined so that its absolute value is at most unity, gives the frequency variation of the cross correlation arising from an isotropic stochastic background, for separated or nonaligned detectors [$\gamma(f) = 1$ at all frequencies for the colocated detector pair, H1 and H2].

The optimal filter is derived assuming that the intrinsic detector noise is Gaussian and stationary over the measurement time, uncorrelated between detectors, and uncorrelated with and much greater in power than the stochastic GW signal. Under these assumptions, the expected variance σ_Y^2 of the cross correlation is dominated by the noise in the individual detectors, whereas the expected value of the cross correlation Y depends on the stochastic background power spectrum:

$$\sigma_Y^2 \equiv \langle Y^2 \rangle - \langle Y \rangle^2 \approx \frac{T}{2} \int_0^{\infty} df P_1(f) |\tilde{Q}(f)|^2 P_2(f), \quad (3)$$

$$\langle Y \rangle = T \int_0^{\infty} df \gamma(f) S_{\mathrm{GW}}(f) \tilde{Q}(f), \quad (4)$$

where T is the duration of the measurement.

Analysis Details.—The analysis is implemented similarly to the method detailed in Ref. [3]. The data set from a given interferometer pair is divided into equal-length intervals, and the cross correlation Y and theoretical σ_Y are calculated for each interval, yielding a set $\{Y_I, \sigma_{Y_I}\}$ of such values, with I labeling the intervals. This data segmentation is useful for dealing with long-term nonstationarity of the detector noise, by choosing an interval length over which the noise is relatively stationary. The interval length for this analysis is 60 sec. The cross-correlation values are

combined to produce a final cross-correlation estimator Y_{opt} that maximizes the signal-to-noise ratio and has variance σ^2_{opt}:

$$Y_{\mathrm{opt}} = \sum_I \sigma_{Y_I}^{-2} Y_I / \sigma_{\mathrm{opt}}^{-2}, \qquad \sigma_{\mathrm{opt}}^{-2} = \sum_I \sigma_{Y_I}^{-2}. \tag{5}$$

The normalization factor $\mathcal{N}$ is defined such that the point estimate of Ω_α and its standard deviation are given by: $\hat{\Omega}_\alpha = Y_{\mathrm{opt}}/T$, $\sigma_{\Omega_\alpha} = \sigma_{\mathrm{opt}}/T$. (Thus, Y_I, Y_{opt}, and $\mathcal{N}$ all have dimensions of time.)

Before computing the cross correlation, each 60 sec data interval is decimated (from 16 384 to 1024 Hz), high-pass filtered (40 Hz cutoff), and Hann windowed. The windowing step protects against spectral leakage of strong lines that may be present in the data [10], but at the same time a Hann window reduces the effective length of the interval by nearly a factor of 2 (approximately the mean value of the Hann window). To recover the loss in signal to noise, the data intervals are overlapped by 50%, so that each data point receives full weighting in the analysis (except for end effects). This introduces some correlation between the Y_I and σ_{Y_I} for adjacent values of I, complicating the formulas for the optimal estimator and its variance, derivations of which may be found in Ref. [11].

The detectors' strain noise power spectral densities (PSDs) are estimated for each interval in order to calculate the optimal filter $\tilde{Q}(f)$. Welch's modified periodogram method of PSD estimation is used, averaging 58 periodograms formed from 4 sec long, 50% overlapping data windows [10]. The PSD for interval I is formed from the two 60 sec data intervals preceding and following, but excluding the data within, interval I. This technique eliminates a bias (underestimate) in the cross correlation that would otherwise exist, due to nonzero covariance between the $\tilde{s}_1^* \cdot \tilde{s}_2$ cross-spectrum and the corresponding power spectra. However, short-term changes (typically increases) in detector noise may produce outliers, because excess instrumental noise within interval I is not reflected in its PSD. This is addressed by applying a consistency test on σ_{Y_I}: If the σ_{Y_I} calculated using the average of the PSDs for interval $I-1$ and interval $I+1$ as described above differs from that calculated from interval I by more than 20%, the data in interval I are not used in the cross-correlation analysis. Approximately 20% of the data were rejected by this cut.

To compute the cross correlation [Eq. (1)], the raw detector data are calibrated, in the frequency domain, into strain units using interferometer response functions. These functions are calculated once per 60 sec, using a measurement of the response of an interferometer to a sinusoidal calibration force, averaged over 60 sec. The frequency domain values of $\{\tilde{s}_1, \tilde{s}_2\}$, given at a frequency spacing of $1/60$ Hz, are binned to the resolution of the optimal filter (frequency spacing of $1/4$ Hz), and the integrations in Eqs. (1) and (3) are performed for the different $S_{\mathrm{GW}}(f)$.

As was important in the earlier analysis of Ref. [3], frequency bins corresponding to known or potential instrumental correlation artifacts are excluded from the frequency domain integrations. An obvious example of intersite correlations comes from the 60 Hz ac supply lines used to power the detectors. The 60 Hz modulation and its harmonics are present to some degree in the detector electronics and, thereby, infiltrate the strain output signal (as Fig. 1 shows). Between L1 and H1,2, the power lines tend to be well correlated over time scales shorter than $\sim$100 sec, with ever-decreasing correlation over longer times. To exclude the possibility of any residual long-term power line correlation, the (60 Hz, 120 Hz, ...) bins are excluded from the integration.

Another narrow-band source of instrumental correlation stems from imperfections in the detectors' data acquisition systems. The peaks in Fig. 2, at multiples of 16 Hz, were produced by slight but periodic corruption of the data at each site. The data acquisition timing at each site is controlled by clocks synchronized to the 1 pulse-per-second signals produced by global positioning system receivers. The 16 Hz periodicity of the data corruption was controlled by these clocks, resulting in persistent intersite correlations at multiples of 16 Hz. Thus, the (16 Hz, 32 Hz, ...) bins are also excluded from the integration. (After S3, the offending clock modules were identified and the problem was corrected.) For a frequency range of, e.g., 70–250 Hz, the removal of $1/4$ Hz bins at multiples of 60 and 16 Hz corresponds to a loss of $\sim$2% of the total bandwidth.

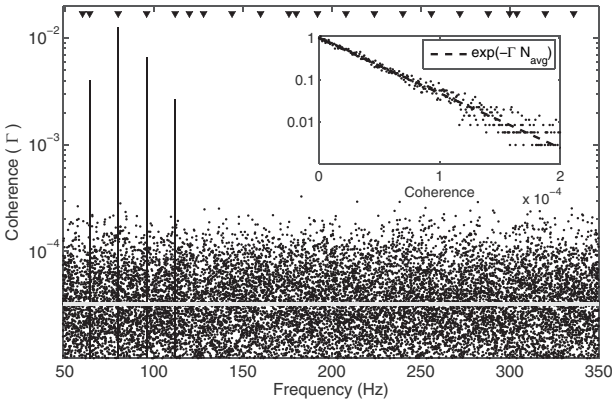

FIG. 2. Coherence between H1 and L1 during S3, showing a few small, but significant, coherent peaks at multiples of 16 Hz. The horizontal line corresponds to the statistical expectation value of $1/N_{\mathrm{avg}} = 3.3 \times 10^{-5}$, where N_{avg} is the number of periodogram averages. The inverted triangles at the top of the graph indicate the discrete frequencies omitted from the analysis. The inset histogram shows that the coherence values (Γ) follow the expected exponential distribution (dashed line).

TABLE I. Results of the cross correlation of LIGO's H1 and L1 interferometers, analyzed for a potential power-law stochastic background of the form: $\Omega_{\rm GW}(f) = \Omega_\alpha (f/100\ {\rm Hz})^\alpha$. The frequency range for each α is the band that contributes 99% of the full sensitivity, as determined by the inverse variance. All results correspond to the specified band and an observation time of 218 h. 90%-confidence Bayesian upper limits on $\Omega_{\rm GW}(f)$ [also expressed as limits on the strain noise density $S_{\rm GW}^{1/2}(f)$] are calculated from the point estimates and statistical errors, marginalizing over a $\pm 11\%$ and $\pm 15\%$ uncertainty in the calibration magnitude of the H1 and L1 detectors.

Power	Frequency	Pt estimate	Statistical error	Calibration error		Upper limits	
law	range	$\hat{\Omega}_\alpha$	σ_{Ω_α}	(H1)	(L1)	$\Omega_{\rm GW}(f)$	$S_{\rm GW}^{1/2}(f)$ (Hz$^{-1/2}$)
$\alpha = 0$	69–156 Hz	-6.0×10^{-4}	7.0×10^{-4}	$\pm 11\%$	$\pm 15\%$	8.4×10^{-4}	$1.2 \times 10^{-23} (f/100\ {\rm Hz})^{-3/2}$
$\alpha = 2$	73–244 Hz	-4.7×10^{-4}	7.2×10^{-4}	$\pm 11\%$	$\pm 15\%$	$9.4 \times 10^{-4} (f/100\ {\rm Hz})^2$	$1.2 \times 10^{-23} (f/100\ {\rm Hz})^{-1/2}$
$\alpha = 3$	76–329 Hz	-4.0×10^{-4}	6.2×10^{-4}	$\pm 11\%$	$\pm 15\%$	$8.1 \times 10^{-4} (f/100\ {\rm Hz})^3$	1.2×10^{-23}

Results.—For each power law searched for, we calculate the optimal cross-correlation statistic and its variance [Eq. (5)]. The H1-L1 results are summarized in Table I. The H2-L1 correlation is approximately a factor of 7 less sensitive than H1-L1, due to the higher noise level of H2; the H2-L1 results are thus not used for the upper limits results (and are not shown), but they are consistent, within their error bars, with the H1-L1 results.

Systematic errors due to unresolved time variations in the interferometers' calibration and power spectra were investigated and determined to be small compared to the statistical error σ_{Ω_α}. Phase calibration uncertainties and timing errors are also negligible. Not negligible are interferometer amplitude calibration uncertainties, estimated as a $\pm 11\%$ ($\pm 15\%$) frequency-independent uncertainty in the strain response magnitude for H1 (L1).

We construct a Bayesian posterior probability distribution for Ω_α using the optimal point estimate $\hat{\Omega}_\alpha$ and statistical error σ_{Ω_α}, marginalizing over the unknown calibration magnitudes (see, e.g., [12]). The prior probability distribution for Ω_α is taken to be uniform from 0 to 0.02 (the maximum value corresponding to the largest background that is still consistent with the lowest single interferometer strain noise); the prior distributions for the calibration magnitudes are taken to be uniform between 1 ± 0.11 (for H1) and 1 ± 0.15 (for L1). The 90% probability upper limit is then that value of Ω_α for which 90% of the posterior distribution lies between 0 and the upper limit. (The upper limit is relatively insensitive to reasonable changes in the priors.) A uniform prior was chosen for Ω_α because of its simplicity and to allow for easy comparison with previous observations. Such a prior favors higher values of Ω_α and, therefore, generates a somewhat more conservative upper limit.

The estimates for Ω_α are entirely consistent with no stochastic background, within the sensitivity of the measurement. Furthermore, the cross-correlation spectrum [i.e., the integrand of Eq. (1)] shows no distinct features (see Fig. 3), and the $\approx 26\,000$ values of Y_I, with mean removed and normalized by the σ_{Y_I}, follow the expected normal distribution.

The data analysis pipeline was validated by checking its performance on fake stochastic signals injected into the data, using a combination of both software and hardware injections [3,13]. The amplitudes of the measured and injected signals agreed to within the statistical error for injections down to a level of $\Omega_0 = 1 \times 10^{-4}$.

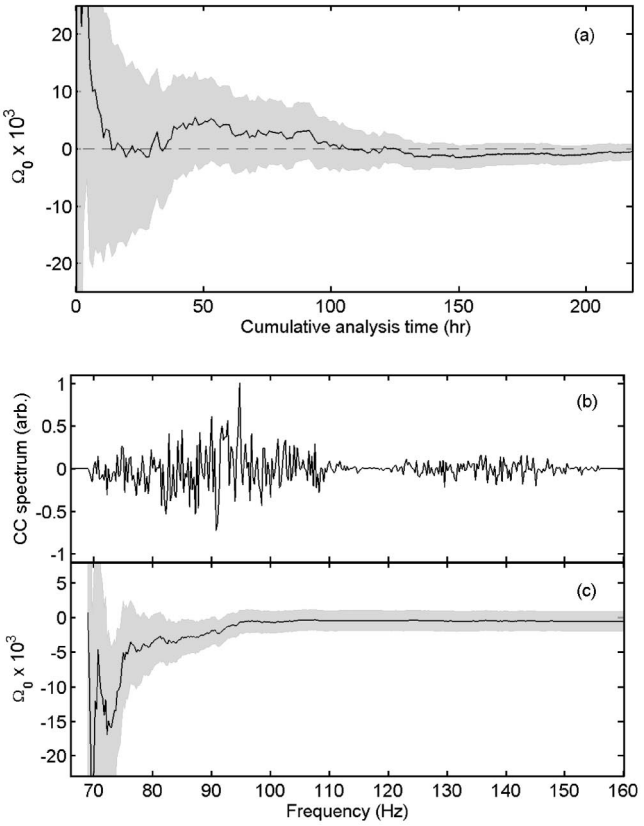

FIG. 3. The estimate $\hat{\Omega}_\alpha$, for H1-L1 and $\alpha = 0$: (a) as a function of the amount of data analyzed. The shaded region shows the $\pm 2\sigma_{\Omega_0}$ band on $\hat{\Omega}_0$. (b) The real part of the H1-L1 cross-correlation spectrum, in arbitrary units. (c) As a function of the frequency range analyzed. The shaded region shows the $\pm 2\sigma_{\Omega_0}$ band on $\hat{\Omega}_0$, cumulative in frequency from 69 Hz to f.

Conclusions.—The energy density in a primordial background of GWs is constrained by big-bang nucleosynthesis theory, giving a conservative bound of: $\int d(\ln f)\Omega_{\rm GW}(f) < 1.1 \times 10^{-5}$ [2]; if all the GW energy were concentrated in our sensitive band, this is still 60× below the limit set here. A background from astrophysical sources would be generated at much later cosmic times and, thus, not be subject to the above bound. In the LIGO band, such a background could be generated by the superposition of many short-lived signals, such as supernova bursts and rotating neutron stars (in the tens to hundreds of hertz band). Uncertainties in the theoretical models are large, though the most optimistic predictions peak at $\Omega_{\rm GW}(f) \sim 10^{-7}$ [2]. Nonetheless, the results presented here provide direct, measured limits to a stochastic background, that, in terms of energy density, are nearly 10^5 lower than previous measurements. Eventually, with 1 year of data at design sensitivity, the LIGO detectors will be sensitive at a level several times below the nucleosynthesis bound.

The authors gratefully acknowledge the support of the United States National Science Foundation for the construction and operation of the LIGO Laboratory and the Particle Physics and Astronomy Research Council of the United Kingdom, the Max-Planck-Society, and the State of Niedrersachsen, Germany, for support of the construction and operation of the GEO600 detector. The authors also gratefully acknowledge the support of the research by these agencies and by the Australian Research Council, the Natural Sciences and Engineering Research Council of Canada, the Council of Scientific and Industrial Research of India, the Department of Science and Technology of India, the Spanish Ministerio de Educacion y Ciencia, the John Simon Guggenheim Foundation, the Leverhulme Trust, the David and Lucile Packard Foundation, the Research Corporation, and the Alfred P. Sloan Foundation.

*Present address: New Mexico State University.
†Present address: Charles Sturt University, Australia.
‡Present address: University of Southampton.
§Present address: New Mexico Institute of Mining and Technology/Magdalena Ridge Observatory Interferometer.
‖Present address: Observatoire de la Cõte d'Azur.
¶Present address: Thirty Meter Telescope Project, Caltech.

[1] C. L. Bennett *et al.*, Astrophys. J. Suppl. Ser. **148**, 1 (2003).
[2] M. Maggiore, Phys. Rep. **331**, 283 (2000).
[3] B. Abbott *et al.*, Phys. Rev. D **69**, 122004 (2004).
[4] P. Astone *et al.*, Astron. Astrophys. **351**, 811 (1999).
[5] J. W. Armstrong *et al.*, Astrophys. J. **599**, 806 (2003).
[6] M. P. McHugh *et al.*, Phys. Rev. D **54**, 5993 (1996).
[7] B. Barish and R. Weiss, Phys. Today **52**, No. 10, 44 (1999).
[8] B. Abbott *et al.*, Nucl. Instrum. Methods Phys. Res., Sect. A **517/1–3**, 154 (2004).
[9] N. Christensen, Phys. Rev. D **46**, 5250 (1992); É. É. Flanagan, Phys. Rev. D **48**, 2389 (1993).
[10] W. H. Press *et al.*, in *Numerical Recipes in C* (Cambridge University Press, Cambridge, England, 1992), Sec. 13.4, 2nd ed.
[11] A. Lazzarini and J. Romano, LIGO Report, 2004, http://www.ligo.caltech.edu/docs/T/T040089-00.pdf.
[12] T. J. Loredo, in *Maximum Entropy and Bayesian Methods*, edited by P. F. Fougère (Kluwer Academic, Dordrecht, 1990).
[13] S. Bose *et al.*, Classical Quantum Gravity **20**, S677 (2003).